Journal of Environment and Earth Science
ISSN 2224-3216 (Paper) ISSN 2225-0948 (Online)
Vol.6, No.6, 2016
www.iiste.org

# New Discovery of Fe - Mn Mineralization along Abu Asal Fault Dead Sea Area, Central Jordan

Hashem Al-Zubi
Ministry of Energy & Mineral Resources; P.O. Box: 140027; AMMAN 11814, JORDAN

**Abstract**
This work is describing a new discovery of iron - manganese deposit in central Jordan. The geology and mineralogy of Lower Cretaceous Kurnub sandstone hosted Fe- Mn mineralization in the area of Wadi Abu Asal was investigated. The mineralization is interesting as it's restricted to the Neogene NNE-SSW trending fault zone, which is related and parallel to the major Dead Sea fault system. In addition, it is outcropping in an area that compresses many hot springs and geothermal indications. The vein type mineralization is the dominating feature, which indicated an epigenetic mineralization. The major oxides geochemistry reveals the hydrothermal origin of the ore, were Fe and Mn have negative correlation with Si and Ca, which are the main elements forming the minerals of the hosting rocks. The mineral phases of iron deposit are the goethite and magnetite.
**Keywords:** Fe-mineralization; Jordan, hydrothermal, veins, goethite; magnetite

## 1. Introduction:

Iron deposits were reported in many areas in central and northern areas of Jordan; such as in the mountains bordering the ancient Moab, north of the ancient Edom and near al Kura in the northern west part of Jordan (Forbes, 1972). Additional iron mineralization was discovered during the geological surveys at Jilad, Bieren and west of Amman (Mikbel et al. 1985). The major iron deposit is the Wardah Iron deposit near Ajloun north Jordan. Many workers had proposed the hydrothermal origin for Warda Iron deposits (Boom & Lahloub, 1962; Zagorac et al. 1968; Addalo & Alhilali, 1988; Saffarini, 1988; and Saffarini & Abu El-Haj, 1997). Whereas; Al-Malabeh et al. (2008) suggested the speleogene –hypogene as the most likely genetic model for ore formation. Mikbel et al. (1985); suggested hydrothermal origin for West Amman iron mineralization too. Bender (1974); also descriped Warda iron deposit as hydrothermal late magmatic origin. El-Hasan et al. (2001) has noticed a small thin Fe-layers with Cu-layers at Wade Dana, and high Fe concentrations as hematite and geothite associated with high-grade Mn ore at Wade Dabah, all are in Finan area – Wade Araba region. These ores are aged to lower- middle Cambrian and deposited as supergene ores, however its sources is hydrothermal exhalations, (El-Hasan et al. 2008). The variation in Fe/Mn ratio within Wade Dana mineralized area which ranged from 0.006 in the south and 0.40 was also investigated using magnetic methods, the results confirms the presence of hematite as main Fe-oxide mineral associated with Mn oxides (El-Hasan & Lataifeh, 2001). This high iron content within Mn ores at Dabbah site in Wade Dana area was mentioned firstly in (GGM, 1965). Shawabekeh, (1998) mentioned the presences of Fe-oxides and hydroxides along the Hummrat Ma'in fault, that extend few kilometers in E-W trending. The Fe- concentrations are between 16.10-043.8 wt%. This is the first attempt to describe this particular Fe-Mn mineralization in areas adjacent to Dead Sea, and hosted in Lower Cretaceous rocks. Therefore, this work aims to describe its geological, geochemical and mineralogical. And it aimed to elucidate its relationship with the Dead Sea rift system. In addition it aims to determine its source of forming solutions and genesis.

## 2. Study area settings:

### *2.1 Location and Climate*

The study area (Wadi Abu Asal) is located in central Jordan, approximately 50 km south-west of Amman (Fig.1). The area lies between 35°35'44" and 35°36'49" long. E. 31°38'42", 31°37'21", 31°38'26" and 31°39'47" lat. N, as shown in Fig. (1). The site is situated to North of Wade Zarqa Ma'in and can be reached through the main road of Amman-Dead Sea-Aqaba highway and through the connecting road near the Dead Sea shore of the Panorama the Dead Sea to the Ma'in village. The study area site is accessible in all seasons and can be crossed by several tracks. The study area shows a little variation in elevation ranging between 120 m to 200 m a.s.l (above sea level). It has a difference in elevation of approximately 80 m in the northeast of the area. The area is crossed by several tracks, extending from the east to the west. The site is characterized by low to moderate relief and fairly uniform, semi-flat to undulate with hummocky surface in some parts in addition to the presence of a few hills. This Wade has steep to moderate gradients and forms a V-shape with narrow semi-flat bottom separated by low hills. Generally, the direction of the drainage in the area is N-NW and E-W. The most common drainage patterns are ephemeral, meandering and dendritic pattern types. They flow in the winter season only.

The site is typical of an arid climate. Hot and dry in summer seasons, and cold semi-wet in the winter seasons. The annual of rainfall ranges 50-100 mm per annum. Natural vegetation is sparse, limited to low desert bushes and grasses. The temperature ranges between -6°C in winter to approximately 43.2°C in summer seasons. The study area is located in a region that is known of its richness in thermal water. Particularly, the eastern adjacent

 

area at (Khan El-Zabeeb). Where the geothermometric calculations taken from 38 wells indicates maximum temperature exceeding 80 ºC, (Saudi & Sbaie, 2003).

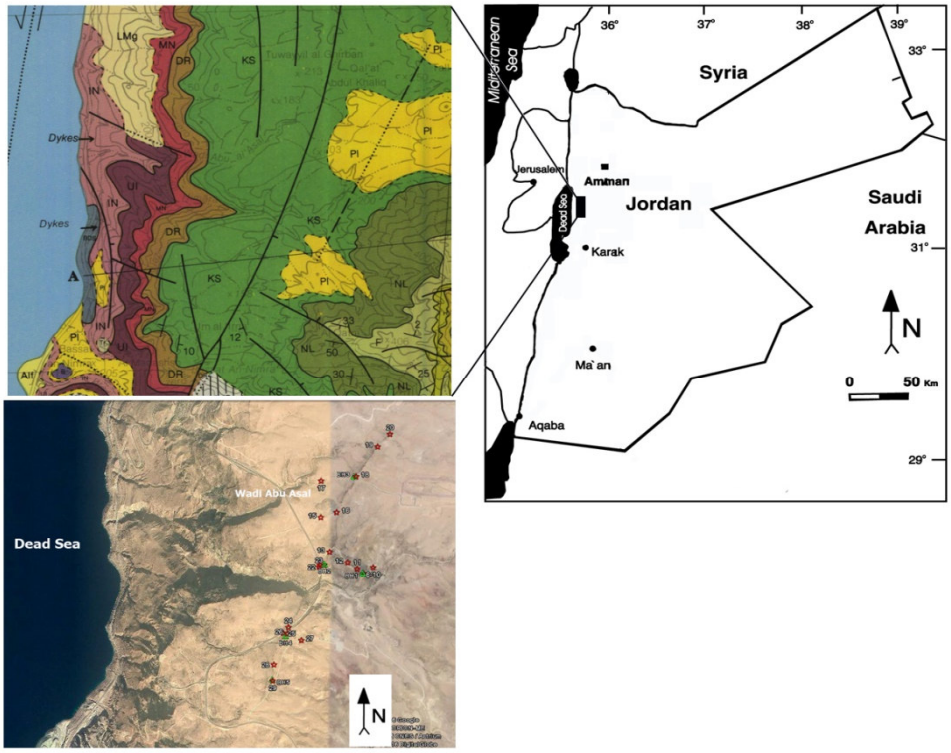


Figure 1. Location map of the study area, with detailed geological map and google earth photos showing the sampling sites.

*2.2 Geological Setting*

Jordan is situated to the north west of the Arabian Peninsula, separated from Palestine by the Dead Sea Rift Valley (Dead Sea Transform) occupied by the Jordan River.

From Cambrian to early Cretaceous, Jordan was located the northern margin of the Gondwana super-continent. The area was relatively tectonically stable during the Paleozoic with dominantly continental sedimentation, and minor but widespread marine incursions. These conditions of sedimentation continued into the early Triassic but by the Late Triassic to early Jurassic the area became increasingly more marine with an open sea lying to the northwest (Ziegler, 2001).

During the late Cretaceous, subduction of the oceanic lithosphere was initiated to the north and resulted in the collision of the Arabian platform with the European continent, associated with folding and obduction of ophiolites (Lovelock, 1984). After this compression event, extension within the Arabian plate during the Late Cretaceous to early Tertiary caused the formation of a series of northwest -trending basins (Bender, 1974; Lovelock, 1984). Later left-lateral strike-slip faulting along the Dead Sea Transform in the Neogene led to the development of well-defined pull-apart basins such as the Dead Sea Basin.

From the Late Cretaceous to Eocene Jordan was covered by an extensive marine transgression from Cenomanian time, in relation with a global warming event, which resulted in the deposition of the Ajlun and Belqa groups (mostly calcareous sediments) (Bender, 1974; Powell and Moh'd, 2011). During the Late Eocene, a regression led to a period of folding, uplift and erosion. This period is also characterized by a left lateral transtensional event which were responsible for the Dead Sea rifting, extensive basalt flows mainly in north-east Jordan, but which extend to Syria and Saudi Arabia, and by localized lacustrine and f1uviatile deposits in the Azraq and Jafr basins (depressions, respectively located at the northeast and southeast of the study area).

The rocks cropping out in the study area mostly sedimentary in origin, and are Cambrian (570-505 Ma), Triassic (225-190 Ma), Cretaceous (144-65 Ma), in age. Paleozoic (Cambrian) rocks crop out in the west of the area adjacent to Dead Sea where they are intruded by dykes. Cambrian siliclastic were deposited by fluvial braided streams. Ordovician, Silurian and Jurassic strata were not deposited or removed by erosion. Although the unconformity between the Cambrian and Triassic is not strongly marked, it represents a time gap of about 225 Ma. The Triassic sequence east of the Rift Valley is about 1000m thick, just 335m crop out in the west of area. These sediments were deposited near the shore, either under terrestrial conditions within the intertidal range just off shore, or under saline conditions in a sabkha lagoon environment. The sedimentary rocks are intruded by dykes and sills

 

composed of diabase and gabbro. The unconformity between Triassic and Cretaceous is not clear. Deposition during the Cretaceous in Jordan was essentially controlled by the balance between transgression of the ocean, situated to the northwest, and uplift and erosion of the Nubo-Arabian shield, to the south, which was the source of continental fluvial siliclastic.

The major fault trends dominate the area. These are E-W-trending Wade Zarqa Ma'in Fault zone it situated south of the study area, and NNE-SSW- trending Dead Sea Fault zone (Rift) which we have the Fe - Mn mineralization along Abu Asal Fault. The fault of Abu Asal Fault movement was late Tertiary in age but the rift probably reflects renewed movements along an ancient weak zone initiated in the late Proterozoic Fig. (1). The iron mineralization are hosted in the lower Cretaceous Kurnub sandstone unit, its age ranged (Neocommian – Cenomanian). The deposits are found as elongated stringers within the NNE-SSW Abu Asal fault, veins and massive impregnated bodies, Fig. (1).

## 3. Sampling and Methodology

Thirty samples were collected along the fault as shown in Fig. (1). the mineral constituents of the samples were determined using x-ray diffraction system (Philips-X` pert MpD). The fine powder samples were randomly mounted on special slides and then scanned between 2◦ and 65◦, using Ni filtered Co K-α- radiation, 40 kv/40mA, divergent and scattering slits of 0.02◦ mm, a receiving slit of 0.15 mm, with stepping of 0.01◦ and scanning speed of 3◦/min. The grain size analysis was done using the laser particle size analyzer (Analysette 22 Compac/ FRISCH). The samples were analyzed for major oxides using a Philips XRF (PHILIPS PW 1404) system, at Ministry of Energy & Mineral Resources (MEMR) laboratories. Analysis according to ASTM C1271-12, LOI according to ASTM C25-11 section 19. The samples were crushed and powdered, then dried at 110 ºC for 2 hours. The analysis of major and trace elements were done by XRF (PHILIPS PW 1404), with an attached 72-position sample changer. Pellets were made by fusing 0.8 g of sample powder and 7.2 g of $L_2B_4O_7$ in Au/Pt crucible using a flexor machine (Leco 2000) for 3 – 4 minutes at 1200 ºC. The melt was poured in a mold and left to cool to form a glass disc and trace elements were analyzed. The machine was calibrated with international standards, particularly the Geological Survey of Japan (GSJ) geochemical standards; (i.e. Japanese slate JSl-1 and JSl-2). The analytical error was within 5%.

## 4. Results and Discussion:

The field outcropping features of iron ores in the study area are very distinctive; mainly the elongation outcrop along the fault, which can be described as structurally-controlled ores. Many epigenetic features are obvious such as the vein mineralization, and impregnated type of ores inside the hosted Kurnub sandstone, some locations showing vertical mineralization along resembling the dyke which might be attributed to the fault plane mineralization. At the cutting sites in the area shows rush mineralization process from the bottom to up along the extension of vertical cracks and fractures. These data confirm the rush process of hydrothermal solutions along the extension of the fault Fig. (2).

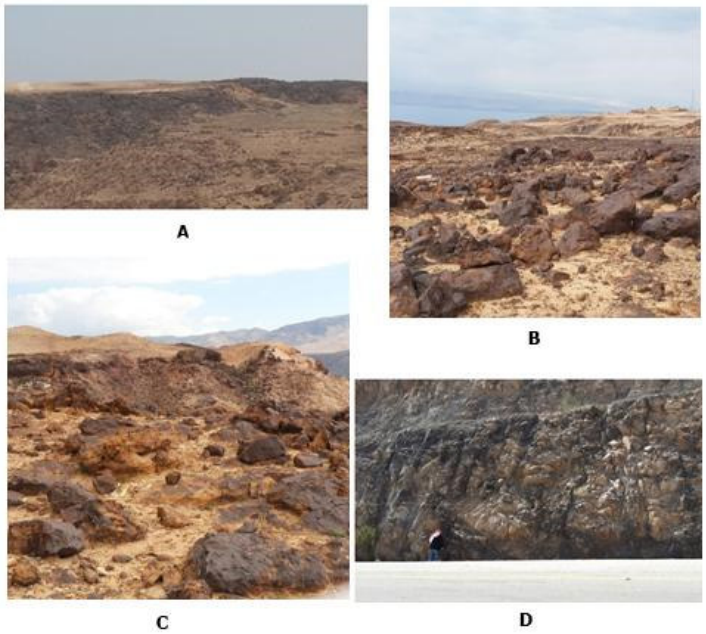


Figure 2. Field photopgraphs A) the closeness of the mineralization site to the Dead Sea; B) The mineralization along Fault plane; C) Impregnated Fe-ores inside the host sandstone rocks; and D) The vein-type mineralization.

 

Moreover, the studied ore geochemical characteristics in terms of the major element composition of the collected samples from Abu Asal deposits. Table (1) shows $Fe_2O_3$ concentrations, ranging from 0.91 to 66.7 wt% with average 17.30 wt% in the rock samples. This wide range of Fe concentration is attributed to the replacement process of the hosting rocks by the epigenetic Fe-solutions. In the same time the main mineral constituent of host rocks $SiO_2$ has also a wide range of concentration (9.43 – 90.9 wt %) with average 24.77 wt%. This can be explained using the correlation coefficient technique as shown in Table (2). This table showed a significant negative correlation was noticed between $Fe_2O_3$ and $SiO_2$ that is equal to (-0.51), and between $Fe_2O_3$ and CaO is equal to (-0.30).

Table 1. XRF analytical results of the studied samples from Wadi Abu Asal (all in Wt%).

| Samples | $Fe_2O_3$ | MnO | $TiO_2$ | CaO | $K_2O$ | $P_2O_5$ | $SiO_2$ | $Al_2O_3$ | MgO | $Na_2O$ | L.O.I | Total |
|---|---|---|---|---|---|---|---|---|---|---|---|---|
| **Asal 1** | 12.1 | 46.2 | 0.78 | 0.42 | 1.41 | 0.45 | 14.9 | 1.81 | 1.05 | 2.79 | 16.4 | 98.31 |
| **Asal 2** | 46.5 | 1.36 | 1.34 | 1.46 | 0.68 | 0.85 | 33.3 | 2.25 | 0.46 | 1.07 | 8.9 | 98.17 |
| **Asal 3** | 66.8 | 6.12 | 0.34 | 2.57 | 0.37 | 0.32 | 9.45 | 0.92 | 0.48 | 0.68 | 12.9 | 100.95 |
| **Asal 4** | 21.5 | 20.6 | 0.65 | 4.98 | 1.43 | 0.68 | 19.8 | 5.54 | 2.3 | 1.95 | 18.8 | 98.23 |
| **Asal 5** | 27.1 | 22.4 | 0.23 | 1.99 | 1.12 | 0.81 | 20.5 | 5.33 | 1.41 | 2.12 | 15 | 98.01 |
| **Asal 6** | 2.68 | 2.83 | 0.02 | 45 | 0.26 | 0.04 | 12.07 | 1.23 | 0.61 | 0.56 | 35.3 | 100.6 |
| **Asal 7** | 54.5 | 0.72 | 0.03 | 1.37 | 0.52 | 0.18 | 22.2 | 5.74 | 0.15 | 1.23 | 10.4 | 97.04 |
| **Asal 8** | 52 | 0.41 | 0.31 | 0.53 | 0.73 | 0.16 | 28.5 | 5.1 | 0.25 | 1.22 | 9 | 98.21 |
| **Asal 9** | 7.33 | 12.4 | 0.67 | 8.31 | 1.97 | 0.67 | 38.7 | 9.36 | 1.97 | 2.04 | 14.7 | 98.12 |
| **Asal 10** | 2.79 | 10.8 | 0.15 | 37.5 | 0.77 | 0.04 | 9.43 | 2.11 | 1.05 | 1.29 | 32.4 | 98.33 |
| **Asal 11** | 11.69 | 16.4 | 0.8 | 3.03 | 1.87 | 1.05 | 43.8 | 6.9 5 | 1.53 | 2.9 | 15.1 | 98.17 |
| **Asal 12** | 28.3 | 6.2 | 0.23 | 2.03 | 0.42 | 0.24 | 50.1 | 2.18 | 0.23 | 1.56 | 6.9 | 98.39 |
| **Asal 13** | 5.1 | 4.06 | 0.05 | 15.2 | 0.22 | 0.16 | 58 | 0.54 | 0.19 | 0.86 | 14.2 | 98.58 |
| **Asal 14** | 12.6 | 3.43 | 0.16 | 3.85 | 0.16 | 0.15 | 71.4 | 0.26 | 0.17 | 0.67 | 5.6 | 98.45 |
| **Asal 16** | 22.6 | 4.64 | 0.28 | 8.22 | 0.27 | 0.43 | 50.1 | 0.97 | 0.34 | 0.76 | 10.4 | 99.01 |
| **Asal 17** | 24.3 | 0.08 | 0.15 | 6.34 | 0.21 | 0.05 | 61.4 | 0.4 | 0.05 | 0.23 | 6.50 | 99.5 |
| **Asal 18** | 0.91 | 3.02 | 0.35 | 2.46 | 0.14 | 0.36 | 88.1 | 0.06 | 0.08 | 0.45 | 2.60 | 98.45 |
| **Asal 19** | 15 | 3.76 | 0.02 | 1.62 | 0.17 | 0.31 | 74 | 0.15 | 0.02 | 0.65 | 3.20 | 98.9 |
| **Asal 20** | 20.6 | 9.24 | 0.07 | 7.19 | 0.54 | 1.69 | 47.5 | 0.94 | 0.55 | 0.38 | 9.20 | 97.9 |
| **Asal 21** | 21.5 | 4.5 | 0.05 | 8.15 | 0.14 | 0.32 | 52.5 | 0.59 | 0.29 | 0.09 | 9.90 | 98.03 |
| **Asal 22** | 3.82 | 10.7 | 0.54 | 1.39 | 0.54 | 0.04 | 75.1 | 0.58 | 0.02 | 0.15 | 5.90 | 98.78 |
| **Asal 23** | 5.48 | 13.9 | 0.04 | 0.64 | 0.71 | 0.11 | 69 | 0.97 | 0.16 | 0.4 | 5.60 | 97.01 |
| **Asal 24** | 0.57 | 2.88 | 0.41 | 0.25 | 0.1 | 0.003 | 90.9 | 0.57 | 0.012 | 0.44 | 3.0 | 99.135 |
| **Asal 25** | 1.02 | 4.12 | 0.33 | 0.65 | 0.1 | 0.015 | 89.8 | 0.014 | 0.034 | 0.02 | 1.90 | 98.003 |
| **Asal 26** | 2.74 | 7.42 | 0.38 | 4.74 | 0.31 | 0.162 | 75.1 | 1.19 | 0.12 | 0.5 | 5.80 | 98.462 |
| **Asal 27** | 19.7 | 13.7 | 0.57 | 6.92 | 0.58 | 0.18 | 45.2 | 0.96 | 0.28 | 0.21 | 9.90 | 98.20 |
| **Asal 28** | 19.4 | 3.97 | 0.76 | 6.12 | 0.15 | 0.1 | 58.8 | 0.47 | 0.18 | 0.35 | 8.80 | 99.10 |
| **Asal 29** | 28.2 | 3.47 | 0.25 | 0.71 | 0.13 | 0.156 | 58.5 | 1.40 | 0.28 | 0.1 | 4.90 | 98.096 |
| **Asal 30** | 22.3 | 3.41 | 0.04 | 10.4 | 0.12 | 0.205 | 49.6 | 0.90 | 0.18 | 0.15 | 10.80 | 98.105 |
| **Min** | 0.91 | 0.72 | 0.02 | 0.25 | 0.1 | 0.003 | 9.43 | 0.01 | 0.012 | 0.02 | 1.90 | 97.01 |
| **Max** | 66.8 | 46.2 | 1.34 | 45 | 1.97 | 1.69 | 90.9 | 9.36 | 2.3 | 2.9 | 35.30 | 100.95 |
| **Average** | 19.28 | 8.61 | 0.34 | 6.69 | 0.56 | 0.34 | 48.64 | 1.88 | 0.50 | 0.89 | 10.83 | 98.50 |
| **St. Dev.** | 17.3 | 9.18 | 0.31 | 10.27 | 0.53 | 0.38 | 24.77 | 2.25 | 0.61 | 0.80 | 7.75 | 0.84 |

Table 2. Correlation Coefficient matrix for the major oxides in the samples of Wadi Abu Asal iron mineralization.

| | $Fe_2O_3$ | MnO | $TiO_2$ | CaO | $K_2O$ | $P_2O_5$ | $SiO_2$ | $Al_2O_3$ | MgO | $Na_2O$ | LOI |
|---|---|---|---|---|---|---|---|---|---|---|---|
| **$Fe_2O_3$** | 1 | -0.19 | 0.09 | -0.3 | -0.006 | 0.16 | -0.51 | 0.29 | -0.02 | 0.09 | -0.07 |
| **MnO** | | 1 | 0.33 | -0.11 | 0.68 | 0.31 | -0.37 | 0.24 | 0.59 | 0.66 | 0.28 |
| **$TiO_2$** | | | 1 | -0.29 | 0.49 | 0.29 | -0.12 | 0.22 | 0.37 | 0.4 | -0.08 |
| **CaO** | | | | 1 | -0.06 | -0.17 | -0.41 | -0.04 | 0.16 | -0.05 | 0.84 |
| **$K_2O$** | | | | | 1 | 0.52 | -0.5 | 0.8 | 0.87 | 0.86 | 0.38 |
| **$P_2O_5$** | | | | | | 1 | -0.27 | 0.31 | 0.52 | 0.44 | 0.07 |
| **$SiO_2$** | | | | | | | 1 | -0.53 | -0.59 | -0.56 | -0.77 |
| **$Al_2O_3$** | | | | | | | | 1 | 0.73 | 0.7 | 0.29 |
| **MgO** | | | | | | | | | 1 | 0.77 | 0.59 |
| **$Na_2O$** | | | | | | | | | | 1 | 0.4 |
| **LOI** | | | | | | | | | | | 1 |

Similarly to lower extent MnO also has negative correlation with $SiO_2$ and CaO (e.g. -037 and -0.11 respectively). This is an indication for replacement nature of mineralization (i.e. epigenetic mineralization). This was better illustrated by the inverse relationship between ($CaO+SiO_2$) versus ($Fe_2O_3+MnO+TiO_2$) as in Fig. (3).

 

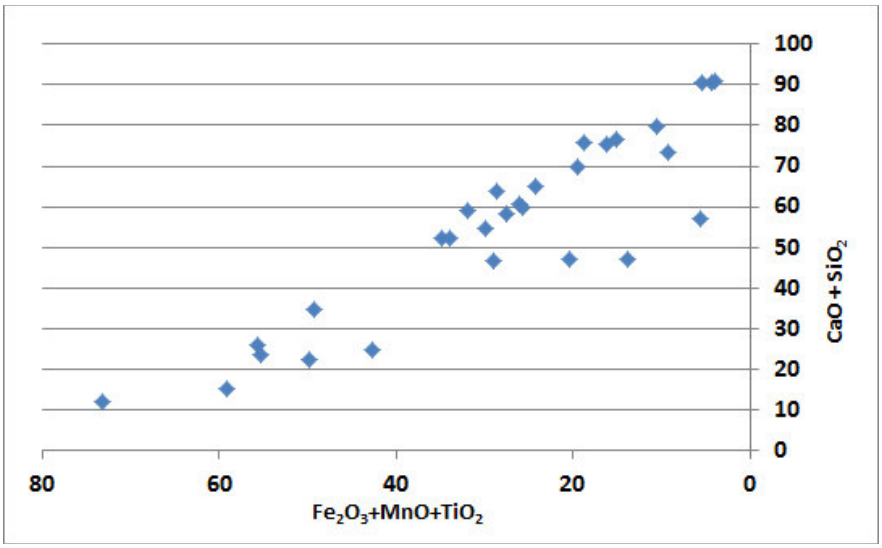


Figure 3. Plotting showing the inverse relationship between the host rock and the Fe-rich solutions.

Comparing it with the main Wardah iron deposit (WID) in northern Jordan it smaller occurrence and has lower Fe content (average 13.48 wt%), whereas WID sediment sample still has average Fe 36.8 wt% (Al-Malabeh et al. 2008). The overall low Mn values are also remarkable for an iron ore, MnO concentration ranges (0.72 – 46.2) with an average 9.18 wt%, and it seems not associated with Fe mineralization due of its slight negative correlation with Fe, Table (2). $Al_2O_3$. Whereas, $K_2O$, $Na_2O$, MgO, $TiO_2$ and $P_2O_5$ are all low in concentrations their average are 0.53 to 0.80, 0.61, 0.31 and 0.38 respectively. The LOI is not entirely water since the Ca and Mg concentrations and therefore considerable $CO_2$ concentrations should be presented. The epigenetic nature of mineralization is determined from the inverse relationship between Kurnub sandstone Unit forming minerals (Quartz and Calcite) and the invading hydrothermal solutions rich elements such as Fe, Mn and Ti. The studied mineralization are uniform with limited Fe/Mn ratio, it characterize with low Fe/Mn ratio as shown in Fe/Mn versus Fe relationship Fig. (4) .this might be indicative for homogeneous single episode of formation by hydrothermal solution passing through fault zone.

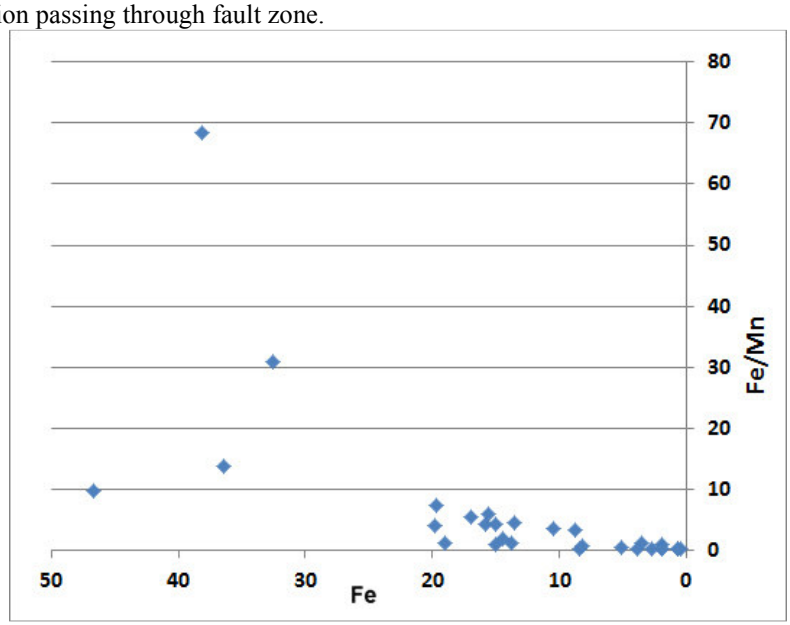


Figure 4. Diagram showing the relationship between Fe and Mn in the ore samples at the studied samples.

Ore mineral constituents was detected using XRD, the results of selected samples are showing in Table (3). The main mineral phases are Quartz and Calcite that represents the host rock. However, Geothite is the main Fe-ore mineral and to lesser extent Magnetite in the studied ore.

 

Table (3): Table summarizing the mineral constituents of host and ore minerals for selective samples from Wade Abu Asal.

| | Q | G | Cc | M |
|---|---|---|---|---|
| Asal 1 | - | * | - | ** |
| Asal 2 | *** | * | - | - |
| Asal 6 | ** | - | *** | - |
| Asal 12 | *** | * | * | - |
| Asal 15 | *** | - | - | - |
| Asal 16 | *** | * | * | - |
| Asal 23 | *** | - | - | - |
| Asal 27 | *** | * | * | - |
| Asal 29 | *** | * | - | - |

*Q: Quartz; G: Geothite; Cc: Calcite; and M: Magnetite*
*(*** Major; ** Minor; * Trace and – Negative)*

This assemblage is typical for hydrothermal origin as reported by many workers (e.g. Saffarini and Abu El-Haj, 1997; Al-Malabeh et al., 2008; El-Hasan et al. 2000). Geothite and magnetite were noticed as the main Fe-minerals in WID hydrothermal ore, (Al-Malabeh et al., 2008).

## 5. Conclusion

From the field views it is very clear that the mineralization zone through the fault extends approximately 4 km in length and with distance about 2 km to the east from the measure Dead Sea fault. This means that the mineralized secondary fault is located on the shear zone of Dead Sea fault.

The Fe - Mn mineralization is hosted in the lower Cretaceous Kurnub sandstone and its outcropping is restricted to NNE-SSW fault zone. It has lower Mn and Ti. Also it has inverse relationship with Si and Ca that representing hosting rock mineral. The field and geochemical features are supporting the hydrothermal origin of the ore. Mineral constituents of the ore are mainly goethite and magnetite which resembling the WID hydrothermal Fe ores.

Further geochemical investigations in terms of trace elements and rare earth elements content in the ore samples is essential to better understand its genesis. Moreover, electrical and gravitational geophysical studies and drilling of exploration wells are needed to delineate the shape, size and the extension of mineralization with the depth.

## 6. Acknowledgment

The author is grateful to the MEMR for providing the laboratories for XRF and XRD analyses, special thanks to fieldwork team of technicians of the geochemical division and the driver, who had a major role in accomplishing this work and for using its vehicles in the field work.

## References:

Addalo, A. & Alhilali, E., (1988), The geochemical study of iron occurrences in the Warda area. - Unpublished report, NRA, Jordan.

Al-Amri. A. Y. (2007), The role of the iron ore deposit of Mugharet el-Wardeh/Jordan in the development of the use of iron in southern Bilad el-Sham, PhD. Thesis. RUHR-UNIVERSTÄT BOCHUM, P184.

Al-Malabeh, A., Kempe, S., Henschel, H.V., Hofmann, H. & Tobschall, H.J. (2008), The Possibly Hypogene Karstic Iron Ore Deposit of Warda near Ajloun (Northern Jordan), its Mineralogy, Geochemistry and Historic Mine. ACTA CARSOLOGICA: 37(2-3): 241-253.

Bender, F., (1974), geology of Jordan. – Bornträger, Berlin, Stuttgart, 196 pp.

Boom, G. van den, & Lahloub, G., (1962), The iron-ore de- posits of Warda in southern Ajloun-District. - Unpublished report.

El-Hasan, T., Al-Malabah, A., and Kumoro, K.: (2008), Rare Earth Elements Geochemistry of the Cambrian shallow marine manganese deposits at Wadi Dana, South Jordan. Jordan Journal of Earth and Environmental Sciences (JJEES). 1(1):45-52.

El-Hasan, T., Al-Malabah, A., Kajiwara, Y., and Komuro, K. (2000), Petrology, Mineralogy, and genesis of Wadi Dana Cambrian Manganese Deposit, Central Wadi Araba Region, Jordan. Qatar University Science Journal. 21:101-117.

El-Hasan, T., and Lataifeh, M. (2001), Differentiation between various manganese deposits of Jordan using magnetization measurments. AL-Manarah, Vol. 7(1): 71-86.

Forbes, R. (1972), Studies in Ancient Technology, Vol. 8, Brill Press, Leiden

Lovelock, (1984), The geological history and structral elements of the Middle East. In: A.E.M. Nairn, A.S.

 

Alsharhan (eds): Sedimentary Basins and Petroleum Geology of the Middle East. Elsevier, Frankfourt, P878.

Mikbel, S., Saffarini, G. & El-Isa, Z., (1985), New iron occurrence west of Amman, Jordan. - Dirasat, 12, 112-124.

Powell, J. and Moh'd, B. (2011), Evolution of Cretaceous to Eocene Alluvial and Carbonate Platform Sequences in Central and South Jordan. GeoArabia, 16, 29-82.

Saffarini, G., & Abu El-Haj, M., (1997), A geochemical soil survey for Fe at Warda iron occurrence, north Jordan. - Abhath Al-Yarmouk, 6(2), 153-157.

Saffarini, Gh.., (1988), Ferride elements abundance in the carbonate-hosted iron occurrences of Jordan. - Dirasat (Science), 15(9): 190-202.

Saudi , A.; and Sbaie, I. (2003), Geochemistry of Thermal Fluids in Central Jordan. Natural Resources Authority Exploration Directorate Geochemistry Division, Unpublished report. Amman. P40.

Shawabekeh, K. (1998), The geology of Ma'in area. Map sheet No. (3153 III). Natural Resources Authority, Bulletin 40. P74. Un-published report.

Zagorac, Z., Karmoul, A. & El-Kaysi, K., (1968), Warda (Ajlun) iron ore deposit, geophysical investigations. Unpubl. Report, NRA, Amman, Jordan, 30 pp.

Ziegler, M. (2001): Late Permian to Holocene Paleo-facies Evolution of the Arabian Plate and its Hydrocarbon Occurrences. GeoArabia, 6(3): 445-505.